A dual-polarized planar 77 GHz array antenna

Stefan Pflüger
Airbus Group Innovations
81663 Munich, Germany
Email: stefan.pflueger@eads.net

Christian Waldschmidt
Ulm University
Institute of Microwave Techniques
89081 Ulm, Germany

Volker Ziegler
Airbus Group Innovations
81663 Munich, Germany

***Abstract*—This paper presents a design approach for a dual-polarized planar antenna array for use within a polarization-agile radar system operating in the frequency range from 76 GHz to 77 GHz. A multilayer stack of organic microwave laminates is used to reach a dense integration of antenna elements and feed lines. This allows to fit individual antenna elements capable of radiating in two orthogonal linear polarizations into a near half-wavelength grid to form a two-dimensional, dual-polarized, planar antenna array.**

I. Motivation

Maneuvering a helicopter at low altitudes over ground while keeping distance to objects like powerlines or trees is a challenging task for the pilot. A radar system tracking these objects could help to prevent severe incidents and thereby increase aviation safety, especially under bad weather conditions.

Radar systems for obstacle detection as presented in [1] often use linear or circularly polarized antennas on a lightweight, cost-effective organic microwave substrate. Earlier publications [2]–[5] in the context of automotive radar suggest that a system capable of switching between arbitrary polarization states potentially offers a higher obstacle detection probability as well as better object classification.

While there is comprehensive literature available on dual-polarized planar E-band antenna elements, few results have been published about the construction of two-dimensional arrays based on these elements. Because of manufacturing process limitations and space requirements for antenna feeding in two polarization modes, most results are limited to single elements ([6], [7]) or one-dimensional linear arrays ([8]). This work presents a concept of a linear antenna array column using a multilayer organic microwave substrate. The width of this column including the feed lines is small enough to be placed side by side to form a two-dimensional planar array antenna.

II. Antenna concept and design

A. Single antenna element

The basic building block of the proposed antenna array is an aperture coupled patch antenna element as shown in Fig. 2. The feed line is placed on the bottom side of a 127 µm thick Rogers RO3003 laminate. Using a slot in the metallization on the top side of this laminate, a small amount of power is coupled to a patch that is placed on a second RO3003 laminate above the slot. While the patch is designed to be resonant at the design frequency, the length of the coupling slot is kept smaller than half the wavelength. Fig. 1 provides an overview of this multilayer setup.

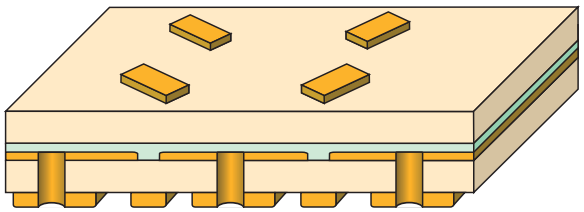

Figure 1. Stackup of the antenna with antenna patches on the top layer, feed lines on the bottom layer and a ground plane with coupling slots in between.

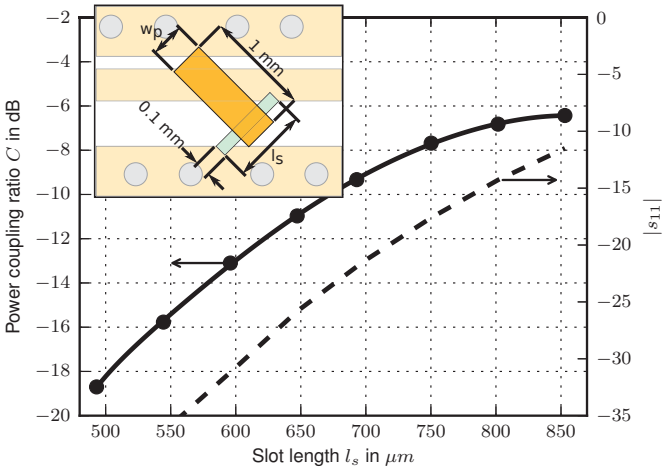

Figure 2. Ratio of radiated power to input power as well as input matching of a single element as a function of slot length l_s at a frequency of 77 GHz.

The ratio of power radiated by the patch to the power fed to the input of the antenna element while terminating its output is further denoted as power coupling ratio $C = P_{\text{rad}}/P_{\text{in}}$. The power coupling ratio C strongly depends on the length l_s of the coupling slot. With stronger coupling, the resonant frequency of the patch drops slightly due to loading of the patch. This is compensated for by a small change of the patch geometry to keep the resonant frequency constant.

Fig. 2 shows the power coupling ratio C determined by full wave simulations for 8 different length values. A polynomial model is fitted to these samples, shown in Fig. 2 as well. This model is used to determine the slot length necessary to realize a predetermined power coupling ratio.

B. Dual-polarized array

A travelling-wave linear array is built by concatenating the antenna elements and terminating one end of the resulting array

ISBN 978-3-8007-3585-3

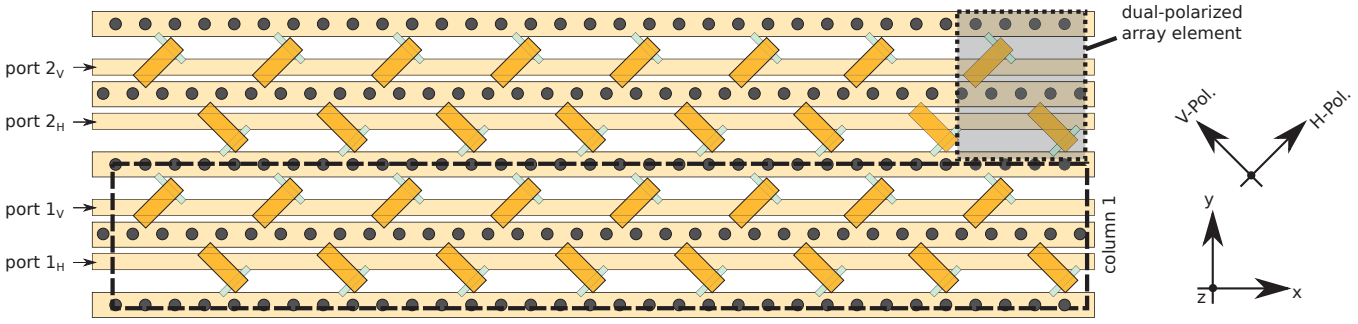

Figure 3. Layout of a 2×8 two-dimensional dual-polarized array. Two columns, eight dual-polarized array elements each, are placed side by side. With reference to the x/y-coordinate system, the direction of vertical (V) and horizontal (H) polarization is rotated by $45°$ as shown on the right.

using a mm-wave absorber. To provide two orthogonal linear polarizations, two of these arrays are joined as shown in Fig. 3 using two separate feed lines.

The low spacial separation between the two feed lines results in mutual coupling. Power coupled to an adjacent feed line is radiated in the wrong polarization and therefore deteriorates the polarization characteristics of the full antenna. A via fence between the feed lines using blind vias is included to minimize this coupling.

Coupling between the patches of different polarization is reduced by arranging them as shown in Fig. 3 within the array columns. The narrow side of the patch, which exhibits maximum E-field strength, is placed along the axis of zero electric field of the surrounding patches and vice versa. If this symmetry is kept, excitation of the resonant patch mode by the adjacent cross-polarized patches is prevented. The positions of the patches between adjacent array columns in Fig. 3 do not fully obey this symmetry because of conflicting grating lobe requirements.

Using the polynomial model developed before, the geometric parameters of the array elements along the array columns are chosen to realize an aperture amplitude distribution that meets specifications concerning side-lobe level, beam-width and array efficiency. Neglecting reflections along the feed line, the power $P_{\text{rad,i}}$ radiated at the i-th antenna element depends on the power coupling ratio as follows:

$$P_{\text{rad,i}} = P_{\text{in}} \cdot C_{\text{i}} \cdot \prod_{j=1}^{i-1} (1 - C_{\text{j}}) \tag{1}$$

From the desired aperture distribution, the value of $P_{\text{rad,i}}$ for each antenna element is known, normalized to P_{in}. Writing Equation (1) for each of the antenna elements results in an equation system that can easily be solved for C_{i}.

The return loss of the array elements for the chosen aperture amplitude distribution is greater than 15 dB. Therefore, this design procedure is expected to yield accurate results although neglecting reflections on the feed line caused by the coupling slots.

Multiple series-fed array columns are placed side by side to form the final, two-dimensional array antenna. This setup is depicted in Fig. 3. As each of the columns is fed independently, electronic beam steering can be used to deflect the beam in the y/z-plane. Deflection of the beam in the x/z-plane may be achieved by different methods including mechanical beam steering or frequency scanning.

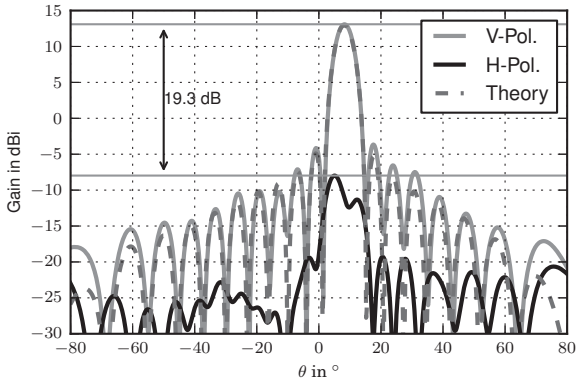

Figure 4. Simulated far-field pattern of an array column in the x/z-plane with excitation of the vertically polarized sub-array. The far-field result is shown in terms of vertical and horizontal polarization as defined by a Ludwig-III coordinate system[9]. The simulation includes loss mechanisms.

III. Results

To verify the design, the far-field characteristics of one series-fed array column with 16 elements are determined by full-wave simulation. The results are presented in Fig. 4. The graph shows the results corresponding to excitation of the input port 1_V in Fig. 3. Referring to the main lobe direction, a cross polarization ratio of 19.3 dB has been reached. The antenna exhibits a side lobe level (SLL) of -16.8 dB.

Fig. 3 additionally shows the theoretically expected pattern by calculating the directivity as a product of element factor and array factor. The array factor can be formulated using the radiated power for each element known from eq. (1), the position of the array elements and the propagation characteristics of the travelling wave feed[10]. The element factor has been approximated using a small dipole model as $\text{EF}(\Theta) = c \cdot \cos(\Theta)$ [11]. To ease comparison of the results, the resulting pattern has been normalized to the gain of the simulation results in Fig. 3. The side lobes of the vertically polarized, simulated pattern match those of the theoretically derived pattern very well. This proves that the aperture amplitude distribution has been implemented as specified, supporting the validity of the design procedure. Small deviations can be explained by the simple element factor model as well as the fact that the calculation

ISBN 978-3-8007-3585-3

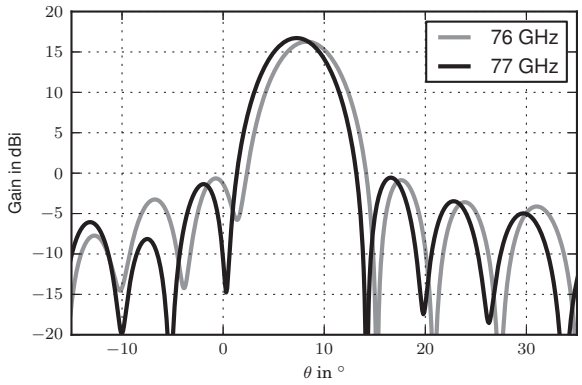

Figure 5. Simulated vertically polarized far-field pattern for two different frequencies. Simulation does not include dielectric or conductive losses.

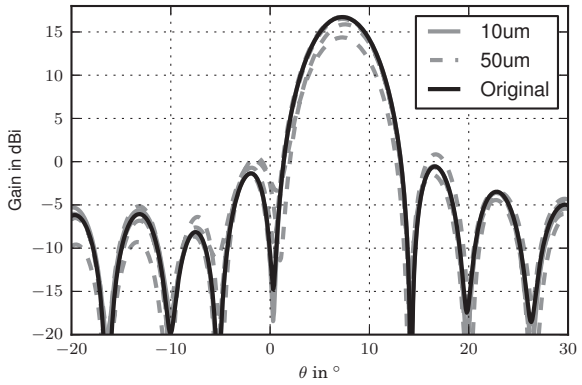

Figure 6. Simulated far-field patterns including a misalignment between the RO3003 cores of 10 µm and 50 µm along the x- and y-axis. Simulation does not include dielectric or conductive losses.

neglects small reflections and coupling effects of the antenna elements.

The antenna has a main beam direction of $\Theta = 7.1°$ at 77 GHz. Because of the spacing between the antenna elements, there is a frequency squint of $1.1°/\text{GHz}$. Fig. 5 illustrates the dependency of the array characteristics on frequency. As the frequency squint is considerably smaller than the 3 dB main beam width of $5.8°$ and the final radar system is specified to work with less than 1 GHz of bandwidth, this is considered to be non-critical.

At mm-wave frequencies, the limitations of the manufacturing processes have to be considered. Several simulations have been carried out to quantify the sensititvity to variations. Small deviations of the size of metallic structures in the range up to 10 µm caused by the etching process do not significantly change the simulation result.

Misalignment of the two RO3003 laminates during the bonding process is another source of error. If the position of the patches or feedlines relative to the slots is changed, the power coupling along the travelling wave array also changes. This leads to a modified aperture distribution that may exhibit a degradation in SLL, gain and beam width. As can be seen from Fig. 6, a misalignment of 50 µm in both the x- and y-axis causes a significant change in the antenna characteristics. This has to be accounted for during system design and yield calculations.

IV. Conclusion

A design approach for a two-dimensional planar antenna array for polarization-agile radar systems has been presented in this paper. It is shown that one-dimensional, dual-polarized arrays, including their feeding structure, can be designed small enough to be placed side by side on multilayer organic microwave laminates. A simplified design procedure based on a concatenation of single antenna elements has been used and validated using EM simulation of a full 16-element linear array.

Based on these one-dimensional linear arrays, a two-dimensional array of arbitrary size can be built. Simulation results show a beam pattern with high directivity and good cross polarization ratio. A nearly half-wavelength spacing of the dual-polarized array elements is possible, which avoids grating lobes in a large scanning range. The sensitivity of the linear array to etching errors and misalignment of the multilayer stack has been evaluated. While narrow tolerances are required, they should be within the capabilities of modern PCB production facilities.

Acknowledgment

This work was supported by the German Federal Ministry of Economics and Technology under contract SITA (#20H0912C).

References

[1] V. Ziegler, F. Schubert, B. Schulte, A. Giere, R. Koerber, and T. Waanders, "Helicopter Near-Field Obstacle Warning System Based on Low-Cost Millimeter-Wave Radar Technology," *Microwave Theory and Techniques, IEEE Transactions on*, vol. 61, no. 1, pp. 658–665, 2013.

[2] A. Britton, "Polarimetric scattering properties of natural targets at 80 GHz," in *Polarisation in Radar, IEE Colloquium on*, 1996, pp. 2/1–2/9.

[3] K. Sarabandi and E. Li, "Effect of radar polarizations on detectability of debris on roads at millimeter-wave frequencies," in *Antennas and Propagation Society International Symposium, 1999. IEEE*, vol. 4, 1999, pp. 2234–2237 vol.4.

[4] J. Schrattenecker, R. Feger, C. Pfeffer, A. Haderer, W. Scheiblhofer, G. Reinthaler, and A. Stelzer, "Polarimetric measurements with integrated sensors at mm-wave frequencies," in *Microwave Conference Proceedings (APMC), 2012 Asia-Pacific*, 2012, pp. 1154–1156.

[5] G. Kulemin, *Millimeter-Wave Radar Targets and Clutter*. Artech House, 2003.

[6] J. A. G. Akkermans and M. H. A. J. Herben, "Millimeter-Wave Antenna With Adjustable Polarization," *Antennas and Wireless Propagation Letters, IEEE*, vol. 7, pp. 539–542, 2008.

[7] K. Thurn, S. Methfessel, and L. Schmidt, "Broadband polarimetric mmWave antennas with differential stripline feed," in *Antennas and Propagation (EUCAP), 2012 6th European Conference on*, 2012, pp. 3529–3532.

[8] B. Porter, L. Rauth, J. Mura, and S. Gearhart, "Dual-Polarized Slot-Coupled Patch Antennas on Duroid with Teflon Lenses for 76.5-GHz Automotive Radar Systems," *Antennas and Propagation, IEEE Transactions on*, vol. 47, no. 1, pp. 1836–1842, 1999.

[9] A. Ludwig, "The definition of cross polarization," *Antennas and Propagation, IEEE Transactions on*, vol. 21, no. 1, pp. 116–119, 1973.

[10] S. J. Orfanidis, "Electromagnetic waves and antennas," http://www.ece.rutgers.edu/%7Eorfanidi/ewa/, 2008.

[11] R. C. Hansen, *Phased Array Antennas (Wiley Series in Microwave and Optical Engineering)*. Wiley-Interscience, 1998.

ISBN 978-3-8007-3585-3